Structural Characterization of Organometallic Sandwich Intercalates of Tin and Zirconium Dichalcogenides by X-ray and Neutron Diffraction and Solid State ^2H NMR Spectroscopy

Heng-Vee Wong, John S. O. Evans, Stephen Barlow, Susan J. Mason, and Dermot O'Hare*

Inorganic Chemistry Laboratory, University of Oxford, South Parks Road, Oxford OX1 3QR, U.K.

Received April 28, 1994[⊗]

The orientations of organometallic sandwich complexes $Co(\eta\text{-}C_5H_5)_2$, $Cr(\eta\text{-}C_5H_5)_2$, $Co(\eta\text{-}C_5H_4CH_3)_2$, $Mo(\eta\text{-}C_6H_6)_2$, $W(\eta\text{-}C_7H_7)(\eta\text{-}C_5H_4CH_3)$, and $Ti(\eta\text{-}C_8H_8)(\eta\text{-}C_5H_5)$ intercalated in the lamellar metal dichalcogenide lattices ZrS_2 and SnX_2 (X = S, Se) have been examined using 1-dimensional refinements of their neutron and X-ray diffraction spectra. The results strongly suggest that these organometallic sandwich complexes all adopt a preferred orientation in which their metal-to-ring centroid axes lie parallel to the host layer planes. The orientation of $Co(\eta\text{-}C_5D_5)_2$ intercalated in ZrS_2 and $SnSe_2$ has been confirmed by solid state ^2H NMR spectroscopy using oriented single crystals of $ZrS_2\{Co(\eta\text{-}C_5D_5)_2\}_{0.25}$ and $SnSe_2\{Co(\eta\text{-}C_5D_5)_2\}_{0.30}$.

Introduction

Despite the initial discovery of organometallic intercalates of the metal chalcogenides almost two decades ago,[1] the full structural refinement of these layered materials has not been achieved. Many of these intercalates demonstrate interesting electronic properties; in particular, $TaS_2\{Cr(\eta\text{-}C_5H_5)_2\}_{0.25}$ and $SnSe_2\{Co(\eta\text{-}C_5H_5)_2\}_{0.3}$ are low-T_c superconductors.[2-4] However, the absence of adequate structural information on these materials has prevented detailed theoretical calculations on their electronic band structures and hindered efforts to understand their observed electronic properties.

Although the structures of alkali metal intercalates of metal dichalcogenides are relatively well understood, the intercalates containing nonspherically symmetric guest molecules have an extra level of complexity: the orientation of the guest molecules in the interlamellar space. This complexity has meant that studies reporting both the orientation of the guest molecules and the lattice sites they adopt have been rare. Perhaps the best understood molecular intercalates of the metal dichalcogenides have been the ammonia and pyridine intercalates of TaS_2, where it was found by neutron scattering,[5,6] X-ray diffraction,[7] and NMR[8,9] studies that the nitrogen atom is located in the center of the van der Waals gap and, in the case of pyridine, that the plane of the aromatic ring lies perpendicular to the sulfide layers. This contradicts the original assumption that the nitrogen lone pair pointed directly toward the layers for maximal orbital overlap with the host bands. Schöllhorn *et al.* subsequently showed that this disposition of the nitrogen lone pairs is favored because the intercalates contain a proportion of ammonium or pyridinium ions which interact via hydrogen bonds with the neutral amine within the guest layer plane.[6,10,11] The structure of the ammonia intercalate of TiS_2 was recently investigated by powder neutron diffraction, which showed the coexistence of ND_3 and spherically disordered ND_4^+ groups in trigonal prismatic interlamellar sites.[12] Further evidence for the orientation of pyridine has been provided by McDaniel *et al.*, who examined the dynamics of the ring rotation in both TaS_2[13] and $CdPS_3$[14] using solid state ^2H NMR.

For the metallocene intercalates however, the guest orientation has been the subject of an unresolved debate for nearly two decades[15-19] with different orientations of the guest molecules reported for different host metal dichalcogenides and indeed even within the same host (TaS_2) at differing temperatures.[17] The two extreme orientations proposed for metallocene molecules in these layered lattices are shown in Figure 1.

Dines[1] initiated the controversy on the metallocene orientation within the host layers when he related the observed increases in interlamellar separation to approximate dimensions of the cobaltocene molecule. He reasoned that increases in the *c*-axis dimension of *ca.* 5.3 Å, taken with the approximation of a cobaltocene molecule as a cylinder of *ca.* 5.65 × 6.8 Å^2, suggested that the guests adopt an orientation with their C_5 axis parallel to the layers. These guest dimensions were, however, later shown to be erroneous in that they underestimate the size of the true van der Waals surface of a metallocene molecule; unsubstituted metallocenes are, as shown by Figure 3, essentially spherical. Some support for the inference of the parallel guest orientation from the observed lattice expansion can, however, be obtained from the crystal structure of pure cobaltocene[20] in

[⊗] Abstract published in *Advance ACS Abstracts,* October 15, 1994.

(1) Dines, M. B. *Science* **1975**, 1210.
(2) Gamble, F. R.; Thompson, A. H. *Solid State Commun.* **1978**, *27*, 379.
(3) Formstone, C. A.; Kurmoo, M.; Fitzgerald, E. T.; Cox, P. A.; O'Hare, D. *J. Mater. Chem.* **1991**, *1*, 51. O'Hare, D.; Wong, H. V.; Hazell, S.; Hodby, J. W. *Adv. Mater.* **1992**, *4*, 658.
(4) Whittingham, M. S. *Mater. Res. Bull.* **1978**, *13*, 775–82.
(5) Riekel, C.; Schöllhorn, R. *Mater. Res. Bull.* **1976**, *11*, 369–76.
(6) Riekel, C.; Hohlwein, D.; Schöllhorn, R. *J. Chem. Soc., Chem. Commun.* **1976**, 863.
(7) Chianelli, R. R.; Scanlon, J. C.; Whittingham, M. S.; Gamble, F. R. *Inorg. Chem.* **1975**, *14*, 1691.
(8) Gamble, F. R.; Silbernagel, B. G. *J. Chem. Phys.* **1975**, *63*, 2544.
(9) Silbernagel, B. G.; Dines, M. B.; Gamble, F. R.; Gebhard, L. A.; Whittingham, M. S. *J. Chem. Phys.* **1976**, *65*, 1906.
(10) Schollhörn, R.; Zagefka, H. D. *Angew. Chem., Int. Ed. Engl.* **1977**, *16*, 199.
(11) Schollhörn, R.; Zagefka, H. D.; Butz, T.; Lerf, A. *Mater. Res. Bull.* **1979**, *14*, 369.
(12) Young, V. G.; McKelvy, M. J.; Glausinger, W. S.; Von Dreele, R. B. *Solid State Ionics* **1988**, *26*, 47.
(13) McDaniel, P. L.; Barbara, T. M.; Jones, J. *J. Phys. Chem.* **1988**, *92*, 626.
(14) McDaniel, P. L.; Liu, G.; Jones, J. *J. Phys. Chem.* **1988**, *92*, 5055.
(15) Silbernagel, B. G. *Chem. Phys. Lett.* **1975**, *34*, 298.
(16) Clement, R. P.; Davies, W. B.; Ford, K. A.; Green, M. L. H.; Jacobsen, A. J. *Inorg. Chem.* **1978**, *17*, 2754.
(17) Heyes, S. J.; Clayden, N. J.; Dobson, C. M.; Green, M. L. H.; Wiseman, P. J. *J. Chem. Soc., Chem. Commun.* **1987**, 1560.
(18) Grey, C.; Evans, J. S. O.; O'Hare, D.; Heyes, S. *J. Chem. Soc., Chem Commun.* **1991**, 1380–2.
(19) O'Hare, D.; Evans, J. S. O. *Comments Inorg. Chem.* **1993**, *14*, 155.
(20) Bunder, W.; Weiss, E. *J. Organomet. Chem.* **1975**, *92*, 65.

0020-1669/94/1333-5515$04.50/0

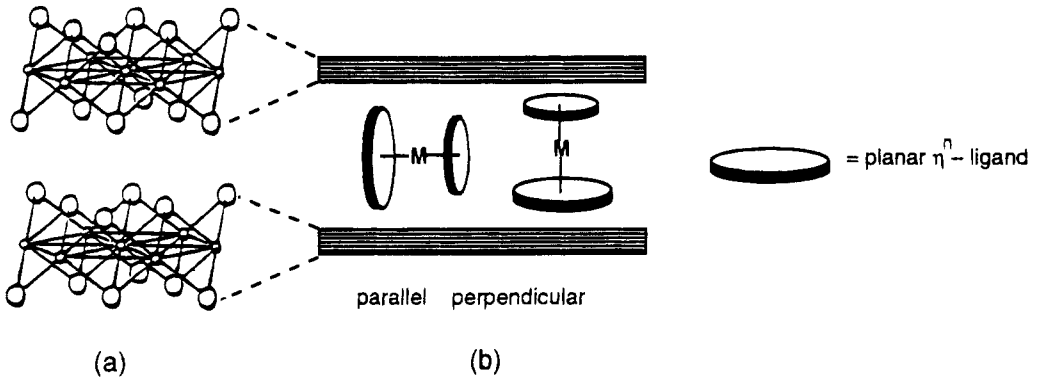

Figure 1. (a) The layered (CdI_2) structure of $SnSe_2$ and ZrS_2. Guest molecules can intercalate the van der Waals gap between the layers. (b) The two possible extreme orientations of a metallocene molecule in a layered host lattice, with its C_5 molecular axis either *parallel* or *perpendicular* to the host lattice layers.

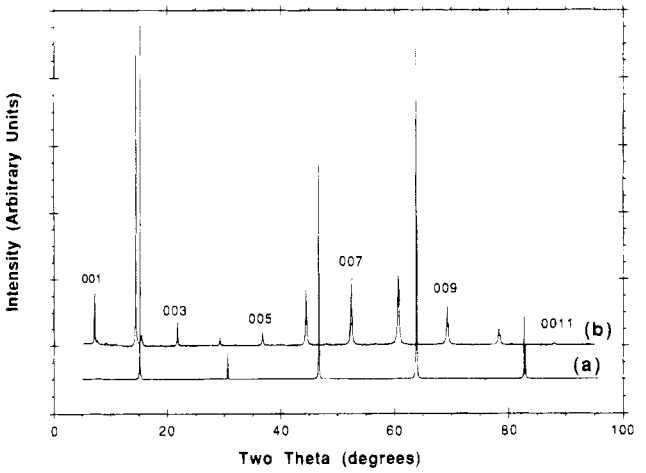

Figure 2. X-ray diffraction spectra of (a) pristine ZrS_2 and (b) ZrS_2-$\{Ti(\eta\text{-}C_8H_8)(\eta\text{-}C_5H_5)\}_{0.2}$.

which the molecules are found to be closely packed in, and have their principal molecular axis parallel to, the 100 plane. The crystallographic distance between these planes is *ca.* 5.05 Å, which correlates reasonably with the observed lattice expansions.

Silbernagel's ^1H NMR study on $TaS_2\{Co(\eta\text{-}C_5H_5)_2\}_{0.25}$ supported the work of Dines and concluded that the C_5 axis of $Co(\eta\text{-}C_5H_5)_2$ lies parallel to the layers.[15] Further evidence for the parallel orientation came from Green and co-workers, who found that an increase in guest ring diameter from $Cr(\eta\text{-}C_5H_5)_2$ to $Cr(\eta\text{-}C_5H_5)(\eta\text{-}C_6H_6)$ to $Cr(\eta\text{-}C_5H_5)(\eta\text{-}C_7H_7)$ caused an increase in interlamellar separation of the ZrS_2 intercalates and no significant change in guest occupancy.[16,21] However, in the same study, he found that substituted bis(arene)molybdenum intercalates showed similar lattice expansions for $Mo(\eta\text{-}C_6H_6)_2$, $Mo(\eta\text{-}C_6H_5CH_3)_2$ and $Mo(\eta\text{-}C_6H_3(CH_3)_3)_2$ but very different guest occupancies, suggesting that here the guest molecules adopt the perpendicular orientation.

Evidence as to the orientation of guest molecules has also been obtained by ^2H NMR studies of deuterated metallocene intercalates. From the temperature dependence of the powder line shape of the ^2H NMR spectrum of $TaS_2\{Co(\eta\text{-}C_5H_5)_2\}_{0.25}$, Heyes *et al.* suggested that the guest molecules can adopt both orientations between the host lattice layers.[17] Their data were interpreted as being due to the fact that solely the perpendicular orientation was present at temperatures below *ca.* 230 K but that a significant proportion of the guest molecules reorient and adopt the parallel orientation at higher temperatures. This interpretation clearly differs from that of Silbernagel. In contrast, $SnS_2\{Co(\eta\text{-}C_5D_5)_2\}_{0.3}$ was shown, both by single-crystal ^2H NMR studies[18] and by X-ray and neutron diffraction experiments,[22] to contain solely $Co(\eta\text{-}C_5H_5)_2$ molecules with their C_5 axes parallel to the *ab* plane.

The primary problem in structural characterization of organometallic intercalates is the high degree of disorder inherent in the *ab* plane of the crystals, resulting in broad peaks for the non-00*l* reflections of their diffraction patterns. As a result, traditional methods of crystal structure determination have not been generally applicable to these systems and, to date, only one full structural study has been attempted, by manually indexing and extracting intensity information from Weissenberg diffraction photographs.[22] This study demonstrated conclusively that the cobaltocene resides with its principal molecular axis parallel to the host layers, but its labor-intensive nature precluded the technique from being used to examine the guest orientations in a wider range of organometallic intercalates.

While a full structural determination is time-consuming and not always possible, 1-dimensional refinement of both X-ray and neutron diffraction data along the *c* axis is a convenient and useful method for ascertaining the guest orientation, especially when aligned samples can be used to collect exclusively 00*l* reflections. Since there is considerably more order in organometallic intercalates along the *c* axis than in the *a* or *b* direction, one can, by aligning several large crystals of the intercalates appropriately, collect solely the sharp, intense 00*l* reflections. From the integrated intensities of these reflections it is possible to calculate 1-dimensional electron density or neutron scattering density profiles, which can be used to deduce the orientation of the guest molecule. The method has been applied by previous researchers in isolated cases such as $TaS_2(Fe_6S_8(PEt_3)_3)_{0.05}$[23] and $SnS_2(Co(\eta\text{-}C_5H_5)_2)_{0.3}$.[22]

This paper describes a systematic study of the orientation of various organometallic sandwich complexes intercalated in ZrS_2 using both X-ray and neutron diffraction as well as solid state ^2H NMR spectroscopy. The guests vary in size and shape from the prototypical metallocenes $(Co(\eta\text{-}C_5H_5)_2$ and $Cr(\eta\text{-}C_5H_5)_2)$ to the larger, mixed-ring sandwich complexes such as $Ti(\eta\text{-}C_8H_8)(\eta\text{-}C_5H_5)$ and $W(\eta\text{-}C_7H_7)(\eta\text{-}C_5H_4CH_3)$. In addition, the $Co(\eta\text{-}C_5D_5)_2$ orientation in ZrS_2 and $SnSe_2$ has been examined by a series of ^2H NMR experiments on the deuterated intercalates $ZrS_2\{Co(\eta\text{-}C_5D_5)_2\}_{0.25}$ and $SnSe_2\{Co(\eta\text{-}C_5D_5)_2\}_{0.3}$.

(21) Davies, W. B.; Green, M. L. H.; Jacobson, A. J. *J. Chem. Soc., Chem. Commun.* **1976**, 781.

(22) O'Hare, D.; Evans, J. S. O.; Wiseman, P. J.; Prout, C. K. *Angew. Chem., Int. Ed. Engl.* **1991**, *30*, 1156.

(23) Nazar, L. F.; Jacobson, A. J. *J. Chem. Soc., Chem. Commun.* **1986**, 570.

Table 1. Growth Conditions for Single Crystals of MX_2 (M = Zr, Sn; X = S, Se) Hosts

compd	reacn temp (°C)	growth temp (°C)	transport agent
ZrS_2	900	800	iodine
$SnSe_2$	560	510	iodine
SnS_2	600	530	bromine

Experimental Section

Synthesis of Metal Dichalcogenide Hosts. Microcrystalline ZrS_2 was formed by heating stoichiometric quantities of elemental Zr and S, with a 1% molar excess of S, at 900 °C for 1 week in evacuated, sealed silica ampules.[24] Typically 3.864 g of finely divided Zr wire (99.9%, Aldrich) and 2.774 g of S (99.9%, Aldrich) were loaded into a 10 cm (length) × 1.5 cm (internal diameter) ampule. The purple ZrS_2 so formed had a reddish tinge (ZrS_3) and was therefore ground under a nitrogen atmosphere and reannealed at 900 °C for another week to give a free-flowing, purple-black powder. The purity of the ZrS_2 was checked by powder X-ray diffraction. Small quantities of ZrS_3 impurities, if present, were removed by sublimation at 900 °C in an evacuated silica ampule. Single crystals of ZrS_2 were grown by iodine vapor transport; typically *ca.* 1 g of microcrystalline ZrS_2 was sealed with iodine (4 mg/cm^3 of ampule volume) in an evacuated silica ampule (25 cm × 1.5 cm internal diameter, 10^{-3} Torr) and heated in a three-zone furnace. A linear temperature gradient between 900 and 800 °C was established in the furnace with the ZrS_2 charge sitting in the hot end. The sample was left to transport for 1 week, after which the ampule was cracked open to yield large platelike crystals of ZrS_2 (*ca.* 4 mm × 3 mm × 0.2 mm). The crystals, which hydrolyze slowly in moist air, were handled and stored under dry nitrogen.

The syntheses of SnX_2 (X = S, Se) were based on procedures established by Al-Alamy and Balchin.[25] Stoichiometric quantities of Sn powder (99.9%, Aldrich) and Se pellets or S powder (99.9%, Aldrich) were weighed out into silica ampules, which were evacuated to 10^{-3} Torr and sealed. The mixture was heated at 560 °C for 1 week, ground, and annealed for a further 1 week. SnS_2 was obtained as a golden brown microcrystalline powder whereas $SnSe_2$ was black. The powder X-ray diffraction patterns of the products corresponded closely with those available from the JCPDS-ICDD database (International Centre for Diffraction Data, Swarthmore, PA 19081).

Single crystals were grown by halogen vapor phase transport (Br_2 for SnS_2, I_2 for $SnSe_2$); a stoichiometric mixture of the elements and 4 mg/cm^3 of transport agent, sealed in an evacuated silica ampule, were heated in the appropriate temperature gradient (see Table 1).

Synthesis of Organometallic Guests. All solvents used were predried over anhydrous 4 Å zeolite molecular sieves, before reflux over the appropriate drying agent (Na metal for toluene; Na/K alloy for petroleum ether (bp 40−60 °C); K metal for tetrahydrofuran) and distillation under an atmosphere of dinitrogen. The solvents were stored under N_2 in Young's ampules containing activated zeolite molecular sieves and were thoroughly degassed before use.

Cobaltocene {$Co(\eta$-$C_5H_5)_2$} was synthesized using a modification of existing procedures[26,27] by reaction of sodium cyclopentadienide with anhydrous cobalt(II) bis(acetylacetonate) (99%, Janssen Chimica). Co(η-$C_5H_5)_2$ was purified by sublimation before use. The same procedure was used to synthesize Co(η-$C_5D_5)_2$ except that C_5D_6 was used instead of C_5H_6. C_5D_6 was obtained by five successive deuterium exchanges of 50 cm^3 of C_5H_6 with *ca.* 50 cm^3 of DMSO and 50 cm^3 of 20% (w/v) NaOD in D_2O. The C_5D_6 was then purified by distillation at 35 °C. The extent of deuteration obtained by this method was >95%, as shown by mass spectroscopic analysis of the deuteriocobaltocene.

The synthesis of Co(η-$C_5H_4CH_3)_2$ was analogous to that for Co(η-$C_5H_5)_2$ except that NaC_5H_5 was replaced by $LiC_5H_4CH_3$. Cr(η-$C_5H_5)_2$ was synthesized by a modification of a procedure reported by Kohler[28,29] while Ti(η-C_8H_8)(η-C_5H_5),[30] Mo(η-$C_6H_6)_2$,[31] W(C_7H_7)($C_5H_4CH_3$),[32] and Mo(C_7H_7)($C_5H_4CH_3$)[33] were made by established literature methods.

Synthesis of Large Crystal Intercalates. Large single crystals of host were trimmed using a sharp scalpel to *ca.* 2 mm × 2 mm × 0.2 mm and added to a toluene solution of the desired organometallic species. The reactants were heated to 120 °C, without stirring, for 1 week before washing with several aliquots of toluene and drying *in vacuo*. The resulting crystals all showed a significant visible expansion along the *c* axis and were black. The stoichiometries of the intercalates were determined by C/H/N elemental analyses performed by Oxford Inorganic Chemistry Laboratory Analytical Services and are reported in Table 2.

Collection and Refinement of Diffraction Data. X-ray diffraction patterns of oriented crystal samples were recorded in Bragg−Brentano (reflection) geometry on a Phillips PW1729 diffractometer, driven by a PW1710 controller interfaced to a microcomputer running Phillips APDv3.5 software. Cu Kα radiation (λ = 1.5418 Å) was used throughout. Thirteen-hour step scans (0.02°/10 s) between 2θ angles of 4.3 and 90° were used in order to collect 00*l* reflections with good counting statistics. The crystals were loaded under an inert atmosphere into an airtight sample holder. This consisted of Capoten film supported on an aluminum frame onto which the crystals were mounted using a small amount of silicone grease. Using such a setup, only the 00*l* reflections of the material were recorded. Observed peak intensities were corrected for the broad baseline due to the Capoten film and small quantities of silicone grease present, as well as for Lorentz, polarization and absorption factors. The *c*-axis cell parameters for all materials were determined from least-squares analysis of 00*l* reflections (using a Choleski matrix inversion method).

Neutron time-of-flight diffraction spectra of aligned crystal samples of the intercalates were collected on the Liquid and Amorphous Diffractometer (LAD) at the ISIS Spallation Neutron Source of the Rutherford Appleton Laboratory, Didcot, U.K. Using a microscope mounted in a nitrogen atmosphere glovebox, *ca.* 1 g of platelike crystals (2 mm × 2 mm × 0.2 mm) were fixed with epoxy resin onto vanadium foil strips. The foil strips were stacked together into a thin-walled vanadium cylinder which was in turn oriented in the LAD sample chamber such that the 00*l* reflections in the *d*-spacing range 12−3 Å could be successively collected in detector banks 3−7. Raw data were normalized using standard procedures described elsewhere and integrated intensities extracted using the CAILS program.[34] Peaks in overlapping regions from spectra obtained from adjacent detector banks were used to normalize the intensities from separate banks, allowing the extraction of relative intensities for the 001−008 reflections.

The 00*l* intensities, derived from either the X-ray or neutron diffraction experiments, were used to perform subsequent least-squares refinements of the guest orientational parameters. The integrated intensity least-squares refinement procedure employed uses Bessel functions of various radii to model the scattering arising from the torus-shaped electron (or neutron-scattering) density of the rapidly rotating carbocyclic rings of the organometallic guest molecules (Program PJWB[35]). Intensity scale factor, the partitioning of guest occupancies between the two orientations, relative S coordinates (*z*/*c*), and isotropic temperature factors were included in the final cycles of refinement. From the structure factors obtained, F_{00l}, the electron or neutron scattering density along the crystallographic axis were obtained by reverse Fourier transformation.

Solid State ^{2}H NMR Spectroscopy. For solid state ^{2}H NMR spectra, crystals of $SnSe_2${Co(η-$C_5D_5)_2$}$_{0.3}$ and ZrS_2{Co(η-$C_5D_5)_2$}$_{0.25}$ were selected by examination under an optical microscope mounted within a glovebox. Each crystal was fixed between thin plastic spacers and sealed in a 5 mm diameter silica tube under nitrogen with a plug

(24) Balchin, A. A. In *Crystallography and Crystal Chemistry of Materials with Layered Structures*; Levy, F., Ed.; D. Reidel Publishing Co.: Dordrecht, Holland, 1976.
(25) Al-Alamy, F. A. S.; Balchin, A. A. *J. Cryst. Growth* **1977**, *38*, 221.
(26) Wilkinson, G.; Cotton, F. A.; Birmingham, J. M. *J. Inorg. Nucl. Chem.* **1956**, *2*, 95.
(27) Wong, H.-V. D.Phil. Thesis, Oxford University, 1993.
(28) Kohler, F. H.; Prossdorf, W. *Z. Naturforsch.* **1977**, *32B*, 1026.
(29) Fischer, E. O. *Inorg. Synth.* **1960**, *6*, 132.
(30) Van Oven, H. O.; De Liefde Meijer, H. J. *J. Organomet. Chem.* **1969**, *19*, 373.
(31) Fischer, E. O.; Scherer, F.; Stahl, H. O. *Chem. Ber.* **1960**, *93*, 2065.
(32) Green, M. L. H.; Ng, D. K. P. *J. Chem. Soc., Dalton Trans.* **1993**, 17.
(33) Green, M. L. H.; Ng, D. P. K. *J. Chem. Soc., Dalton Trans.*, in press.
(34) David, W. I. F.; Ibberson, R. M. *Powder Diffraction at ISIS*; Rutherford Appleton Laboratory: Didcot, U.K., 1990.
(35) Wiseman, P. J. D.Phil. Thesis, Oxford, University. Full listing in ref 27.

Table 2. Comparison of Lattice Expansions along the *c* Axis for $SnSe_2$ and ZrS_2 Intercalates with the Dimensions of Guest Species (Length and Width Conventions Shown in Figure 2)

compd	interlayer spacing (Å)[a]	interlayer expansion (Å)[b]	guest dimension[c]	
			max length (Å)	max width (Å)
$SnSe_2\{Co(\eta\text{-}C_5H_5)_2\}_{0.30}$	11.84(1)	5.70	6.96	6.76
$ZrS_2\{Co(\eta\text{-}C_5H_5)_2\}_{0.25}$	11.23(1)	5.41	6.96	6.76
$ZrS_2\{Cr(\eta\text{-}C_5H_5)_2\}_{0.20}$	11.26(1)	5.43	6.96[d]	6.76[d]
$ZrS_2\{Co(\eta\text{-}C_5H_4CH_3)_2\}_{0.20}$	11.27(1)	5.44	7.90	8.84
$ZrS_2\{W(\eta\text{-}C_7H_7)(\eta\text{-}C_5H_4CH_3)\}_{0.20}$	11.86(3)	6.03		
$ZrS_2\{Mo(\eta\text{-}C_6H_6)_2\}_{0.20}$	11.71(1)	5.88	7.08	7.23
$ZrS_2\{Ti(\eta\text{-}C_8H_8)(\eta\text{-}C_5H_5)\}_{0.20}$	12.20(1)	6.37	6.97	8.15

[a] Obtained by least-squares and refinement of experimental data. [b] Using $c(ZrS_2) = 5.83$ Å and $c(SnSe_2) = 6.14$ Å. [c] Dimensions of un-ionized guests (see Figure 2). [d] Based on $Co(\eta\text{-}C_5H_5)_2$ dimensions.

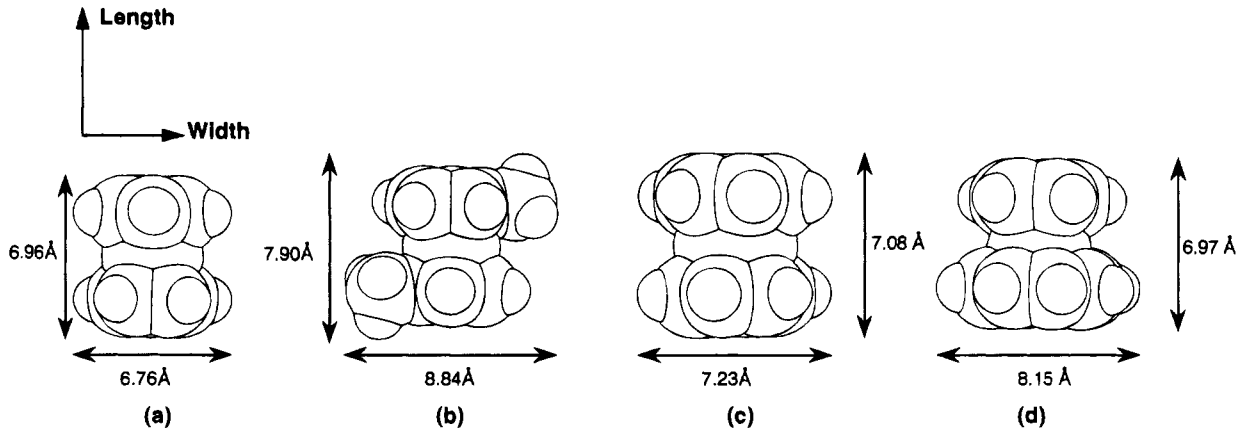

Figure 3. Space-filling models of various organometallic guests showing the van der Waals radii of the constituent atoms: (a) $Co(\eta\text{-}C_5H_5)_2$; (b) $Co(\eta\text{-}C_5H_4CH_3)_2$; (c) $Mo(\eta\text{-}C_6H_6)_2$; (d) $Ti(\eta\text{-}C_5H_5)(\eta\text{-}C_8H_8)$.

of epoxy resin. Spectra of both $SnSe_2\{Co(\eta\text{-}C_5D_5)_2\}_{0.3}$ and $ZrS_2\{Co(\eta\text{-}C_5D_5)_2\}_{0.25}$ were recorded at room temperature with the crystal layers (*ab* plane) oriented perpendicular to the magnetic field on a Bruker MSL400 spectrometer equipped with a high-power probe containing a horizontal solenoid insert. A quadrupolar echo sequence was used, with a spin echo delay of 30 μs, $\pi/2$ pulses of 3 μs, and a relaxation time of 5 s. Further details of the spectrometer setup are described elsewhere.[36]

Results and Discussion

The organometallic molecules $Co(\eta\text{-}C_5H_5)_2$, $Cr(\eta\text{-}C_5H_5)_2$, $Co(\eta\text{-}C_5H_4CH_3)_2$, $Mo(\eta\text{-}C_6H_6)_2$, $W(\eta\text{-}C_7H_7)(\eta\text{-}C_5H_4CH_3)$, and $Ti(\eta\text{-}C_8H_8)(\eta\text{-}C_5H_5)$ can be readily intercalated into the host lattices ZrS_2, SnS_2, or $SnSe_2$ by refluxing a toluene solution of the appropriate guest with a suspension of the powdered metal dichalcogenide for 2−3 days at 120 °C. Large single-crystal samples (ca. 2.0 × 2.0 × 0.2 mm) of the intercalate phase may be obtained by prolonged reflux (1−2 weeks) in toluene at 120 °C without mechanical stirring. The interlayer dimensions of the intercalates (obtained from least-squares analysis of the X-ray data) are listed in Table 2 along with the interlayer expansion (Δc), stoichiometry, and dimensions of the guest molecule. These values compare favorably with those which have been reported previously for polycrystalline materials.[3,16,19,37,38]

X-ray diffraction patterns of aligned single crystals of these intercalates were of high quality. A typical example, that of $ZrS_2\{Ti(\eta\text{-}C_5H_5)(\eta\text{-}C_8H_8)\}_{0.2}$, is shown alongside that of pristine ZrS_2 in Figure 2. Spectra of a similar quality were recorded for all the compounds of Table 2, in which the guest molecules vary in shape from the essentially spherical $Co(\eta\text{-}C_5H_5)_2$ to the larger, truncated cone-shaped $Ti(\eta\text{-}C_5H_5)(\eta\text{-}C_8H_8)$ (Figure 3). From these spectra, it was possible to extract integrated intensities of 00*l* ($l = 1-10$) reflections. Aligned neutron diffraction spectra were also obtained for the $Co(C_5D_5)_2$ and $Cr(C_5D_5)_2$ analogues of the intercalates of Table 2. From these, accurate intensities could be extracted for 00*l* ($l = 1-8$) reflections. Limited access to neutron time and the difficulties in obtaining highly deuterated samples of the other intercalates precluded the recording of further neutron diffraction data.

After the necessary instrumental corrections were applied, the integrated intensities of the 00*l* reflections from either the X-ray or the neutron diffraction patterns were extracted and used for structural refinement. The process of intercalation has been shown to leave the internal structure of the host lattice layers largely undisturbed, such that while the host *c* axis expands considerably on intercalation, the *a* and *b* cell parameters are largely unchanged. For the purposes of 1D refinement, a starting model was therefore used in which metal and sulfur fractional coordinates based on the structures of the pristine host lattices were used to phase the experimental data (typically M at $z/c = 0.0$ and S at $z/c = \pm 0.125$ were used as starting positions). Fourier maps phased on these positions clearly showed scattering density due to the guest molecules in the interlamellar region. Guest molecules were therefore introduced into the model with the metal atom at $z/c = 0.5$ and their principal molecular axes either parallel or perpendicular to the host lattice layers. In successive cycles of refinement, the scale factor, S *z* coordinate, and a parameter which partitioned the proportion of the guest molecule between the two extreme orientations were varied. The overall guest occupancy was fixed at the experimentally observed value obtained from the elemental microanalytical data for the crystals. In all cases, the final proportion of guest molecules in each orientation was found to

(36) Mason, S. J. D.Phil. Thesis, Oxford University, 1993.
(37) Benes, L.; Votinsky, J.; Lostak, P.; Kalousova, J.; Klikorka, J. *Phys. Status Solidi A* **1985**, *89*, K1.
(38) Votinsky, J.; Benes, L.; Kalousova, J.; Lostak, P.; Klikorka, J. *Chem. Pap.* **1988**, *42*, 133.

Table 3. Summary of the Final Least-Squares Parameters Derived from the X-ray and Neutron Diffraction Data

	X-ray					neutron				
compd	S/Se coord (z/c)	parallel[a] occ	perpend[a] occ	% parallel bcc	R factor (%)[b]	S/Se coord (z/c)	parallel[a] occ	perpend[a] occ	% parallel occ	R factor (%)
$SnSe_2\{Co(C_5H_5)_2\}_{0.30}$	0.134(1)	0.29(2)	0.01(2)	97	1.79	0.126(4)	0.291(7)	0.009(7)	97	8.15
$ZrS_2\{Co(C_5H_5)_2\}_{0.25}$	0.136(1)	0.24(1)	0.01(1)	96	1.42	0.126(4)	0.242(5)	0.008(5)	97	5.63
$ZrS_2\{Cr(C_5H_5)_2\}_{0.20}$	0.137(0.4)	0.18(1)	0.02(1)	90	1.28	0.129(4)	0.202(8)	−0.002(8)	100	5.05
$ZrS_2\{Co(C_5H_4CH_3)_2\}_{0.20}$	0.135(1)	0.17(2)	0.03(2)	85	3.39					
$ZrS_2\{W(C_7H_7)(C_5H_4CH_3\}_{0.20}$	0.133(2)	0.16(5)	0.04(5)	80	3.51					
$SnS_2\{W(C_7H_7)(C_5H_4CH_3\}_{0.30}$	0.133(3)	0.21(3)	0.09(3)	70	5.20					
$ZrS_2\{Mo(C_6H_6)_2\}_{0.20}$	0.122(2)	0.19(2)	0.01(2)	95	2.70					
$ZrS_2\{Ti(C_8H_8)(C_5H_5)\}_{0.20}$	0.122(0.2)	0.19(1)	0.01(1)	95	1.06					

[a] "Parallel" and "perpend" refer to orientations in which the metal−ring centroid axis lies parallel and perpendicular to the *ab* plane, respectively. [b] R factor is defined as $[\Sigma(I_o - I_c)/(\Sigma I_o)] \times 100$, where I_c are the observed and calculated intensities, respectively.

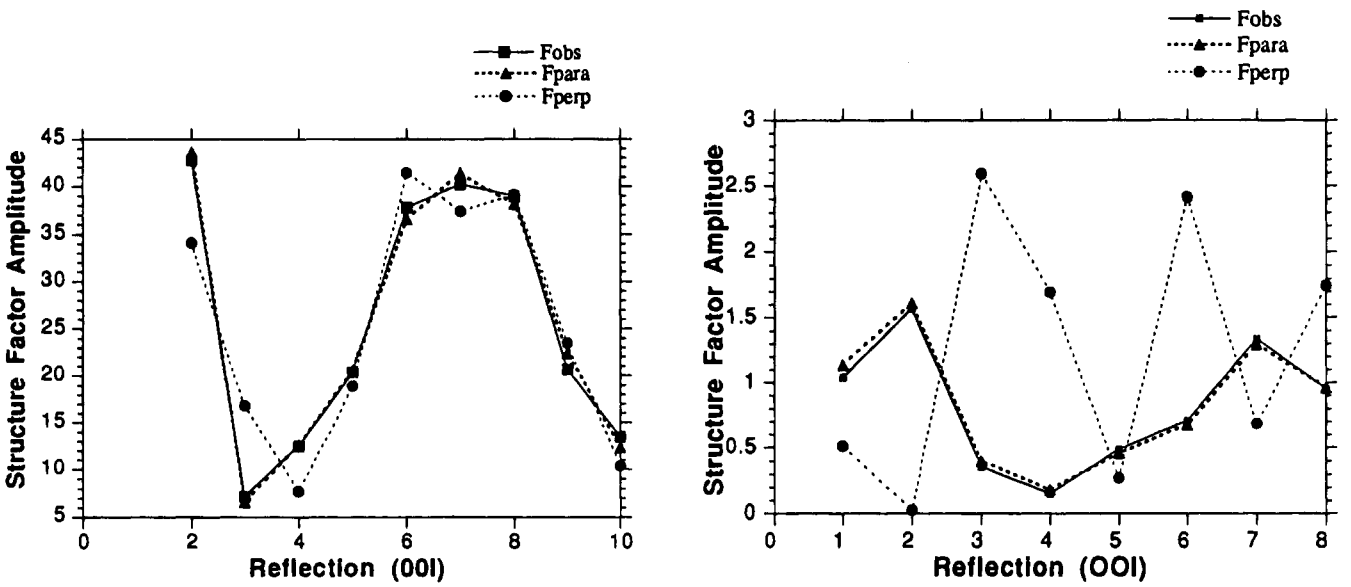

Figure 4. Comparison of experimentally obtained structure factor amplitudes ($|F_{00l}|$) (■) *versus* those calculated from models in which the guests were assumed to be in one of two extreme orientations, that is, with the principal molecular axis parallel (▲) or perpendicular (●) to the host layers: X-ray data (left) and neutron data (right) for $ZrS_2\{Cr(\eta\text{-}C_5H_5)_2\}_{0.2}$ and $ZrS_2\{Cr(\eta\text{-}C_5D_5)_2\}_{0.2}$, respectively.

be independent of the starting model used. The results of the refinements and the guest orientations they suggest for all the intercalate phases studied are shown in Table 3.

As an illustrative example, a comparison of the observed and calculated structure factor amplitudes $|F_{00l}|$ for $ZrS_2\{Cr(\eta\text{-}C_5H_5)_2\}_{0.20}$, using integrated intensity data extracted from both the X-ray and the neutron diffraction patterns, is shown in Figure 4. Figure 4 clearly demonstrates the excellent level of agreement between our experimental data and those determined from a model in which all the cobaltocene molecules were oriented with their C_5 axes parallel to the host layers. Electron and neutron nuclear scattering density plots along the crystallographic c axis have also been calculated for $ZrS_2\{Cr(\eta\text{-}C_5H_5)_2\}_{0.20}$ and are shown in Figure 5.

The standard deviations on the refined X-ray and neutron data indicate that occupancy refinement is more accurate using neutron data, while the S/Se coordinates are more precisely determined by refinement of the X-ray data. The increased precision in the determination of guest orientation using neutrons arises because the structure factor amplitudes $|F_{00l}|$'s computed for each of the two guest orientations in the intercalates are more markedly different for neutron than for X-ray diffraction (see Figure 4). The stronger dependence of the $|F_{00l}|$'s on guest orientation in the case of neutron diffraction can be rationalized by examining the relative contributions of the guest molecule toward the overall X-ray or neutron scattering in these intercalates (see Tables 4 and 5).

In the neutron diffraction experiment, the deuterated cyclopentadienyl ligands of the guest molecules dominate the overall scattering, making neutrons a sensitive probe of guest orientation. In contrast, X-rays are predominantly scattered by the ZrS_2 or $SnSe_2$ host layers and are therefore a more sensitive indicator of the S/Se z coordinate. However, while X-ray diffraction is a less discriminating probe of guest structure than neutron diffraction, comparison of results for $Co(\eta\text{-}C_5H_5)_2$ and $Cr(\eta\text{-}C_5H_5)_2$ in Table 3 shows it is still a *qualitatively* good indicator of guest orientation. Both methods indicate that the organometallic guests reside with their metal−ring centroid axes parallel to the host layers. This finding is supported by data in Table 2 which show that the c-axis expansion increases as a function of the width of the guest, while the length remains essentially constant.

Taken together, the data in Tables 2 and 3 allow us to make several observations about the guest orientation and packing between the layers. The dimensions of $Co(\eta\text{-}C_5H_5)_2$ and $Ti(\eta\text{-}C_5H_5)(\eta\text{-}C_8H_8)$ from ring centroid to ring centroid are roughly the same, as are their stoichiometries in the intercalates. Hence the difference in c-axis expansion can be best explained by the adoption of the parallel guest orientation within host layers. This is confirmed by 1-dimensional refinement of the diffraction data in both cases. In contrast, $Co(\eta\text{-}C_5H_5)_2$ and $Cr(\eta\text{-}C_5H_5)_2$ intercalates of ZrS_2 show virtually the same interlayer expansions. Since they have similar molecular dimensions, the difference in stoichiometry of the intercalates suggests the

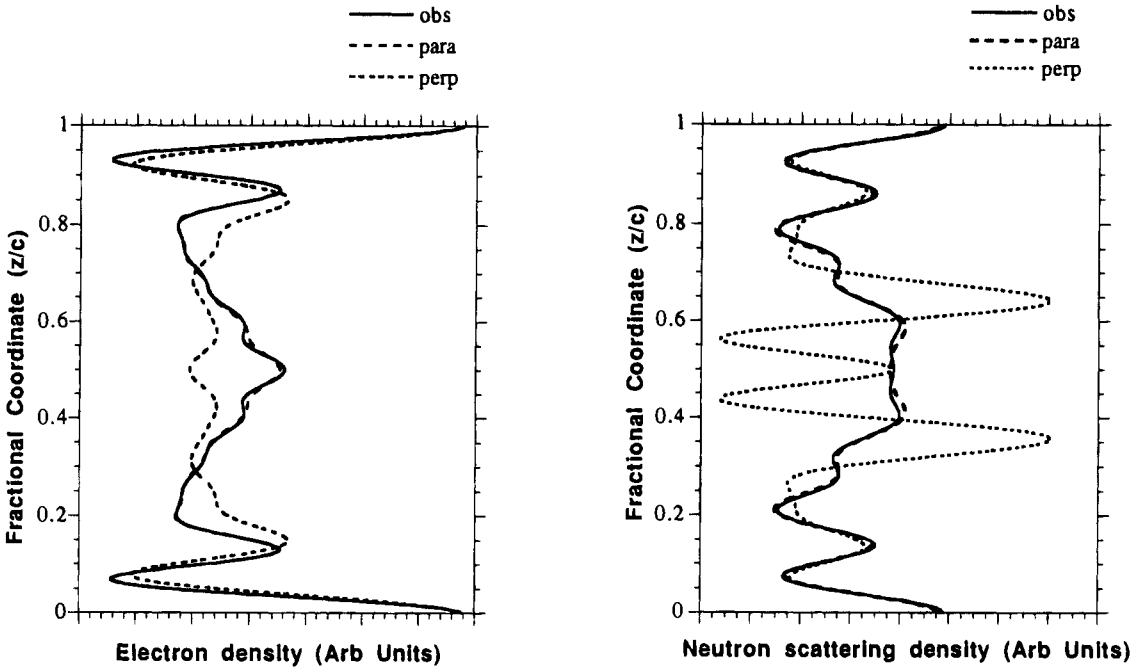

Figure 5. Comparison of 1-dimensional electron and neutron scattering densities along the *c* axis calculated from experimental data (—) versus those calculated from models in which the guests were assumed to be in one of two extreme orientations, that is, with the principal molecular axis parallel (- - -) and perpendicular (• • •) to the host layers: X-ray data (left) and neutron data (right) for $ZrS_2\{Cr(\eta\text{-}C_5H_5)_2\}_{0.2}$ and $ZrS_2\{Cr(\eta\text{-}C_5D_5)_2\}_{0.2}$, respectively.

Table 4. Relative Contributions of the Guest Molecules {G} to Overall Diffraction Intensity in the X-ray Diffraction Patterns of $ZrS_2\{G\}_x$

guest, G	sum of electrons in guest	stoichiometry, x	% contribn
$Co(\eta\text{-}C_5H_5)_2$	97	0.25	25.2
$Cr(\eta\text{-}C_5H_5)_2$	94	0.20	20.7
$Co(\eta\text{-}C_5H_4CH_3)_2$	113	0.20	23.9
$Mo(\eta\text{-}C_6H_6)_2$	126	0.30	34.4
$W(\eta\text{-}C_7H_7)(C_5H_4CH_3)$	166	0.20	31.6
$Ti(\eta\text{-}C_8H_8)(\eta\text{-}C_5H_5)$	113	0.25	28.2

Table 5. Relative Contributions of the Guest Molecules {G} to Overall Diffraction Intensity in the Neutron Diffraction Patterns of $ZrS_2\{G\}_x$

guest, G	sum of guest neutron scattering lengths (10^{-12} cm)	stoichiometry, x	% contribn
$Co(\eta\text{-}C_5D_5)_2$	13.575	0.25	72.5
$Cr(\eta\text{-}C_5D_5)_2$	13.6855	0.20	68.0
$Co(\eta\text{-}C_5D_4CD_3)_2$	17.5742	0.20	73.2
$Mo(\eta\text{-}C_6D_6)_2$	16.681	0.30	79.6
$W(\eta\text{-}C_7D_7)(C_5D_4CD_3)$	17.1282	0.20	72.7
$Ti(\eta\text{-}C_8D_8)(\eta\text{-}C_5D_5)$	16.9748	0.25	76.8

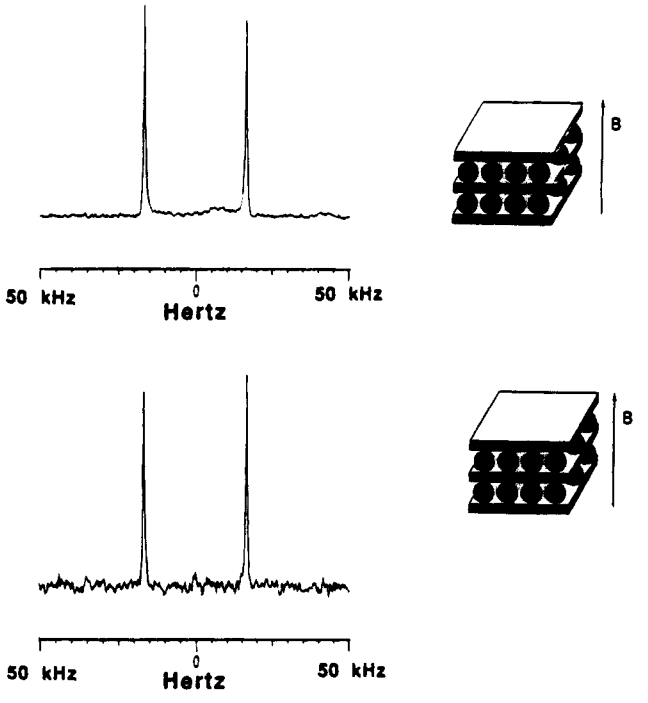

Figure 6. Solid state ^2H NMR spectra of oriented single crystals of $ZrS_2\{Co(\eta\text{-}C_5D_5)_2\}_{0.25}$ (top) and $SnSe_2\{Co(\eta\text{-}C_5D_5)_2\}_{0.3}$ (bottom). The crystals are oriented with their crystallographic *ab* plane perpendicular to the magnetic field.

absence of close packing in $ZrS_2\{Cr(\eta\text{-}C_5H_5)_2\}_{0.20}$. Since $Co(\eta\text{-}C_5H_4CH_3)_2$ is somewhat larger than $Co(\eta\text{-}C_5H_5)_2$ perpendicular to the metal-to-ring centroid axis, it might be expected to induce a significantly larger interlayer expansion upon intercalation into ZrS_2. The observation of essentially identical layer separations for these two compounds together with the lower guest stoichiometry for the substituted intercalate suggests that the methyl substituents lie between the sulfur layers, making the effective guest "width" the same as that for $Co(\eta\text{-}C_5H_5)_2$.

An observation common to all the intercalates studied is that the interlayer expansion is somewhat smaller than the van der Waals dimensions of the guest molecules given in Table 2. This discrepancy can be ascribed to the two following reasons: (a) Since the organometallic guests are ionized upon intercalation into the lattice, there is a net positive charge on the metal center which causes a contraction of the molecule and hence a reduction in its effective van der Waals dimensions. (b) There may be some interpenetration of the C−H or C−D bonds of the carbocyclic rings into the chalcogenide layers, so that the lattice need not expand by the full van der Waals width of the guest molecule.

To provide an independent indication of guest orientation, solid state ^2H NMR spectra of single-crystal samples (*ca.* 1.0 × 1.0 × 0.2 mm^3) of $ZrS_2\{Co(\eta\text{-}C_5D_5)_2\}_{0.25}$ and $SnSe_2\{Co(\eta\text{-}$

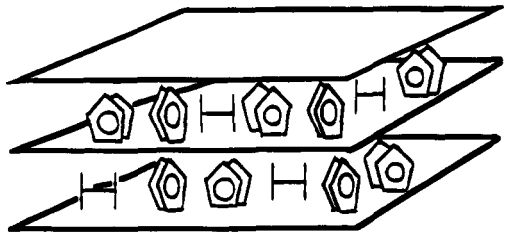

Figure 7. Cobaltocene guests in the van der Waals gap of a lamellar host. Although they all have their principal C_5 axes parallel to the layers, they can adopt a range of orientations in the crystallographic *ab* plane.

$C_5D_5)_2\}_{0.3}$ were recorded. Spectra recorded with the crystals oriented with their crystallographic *ab* plane (i.e. the plane of the layers) perpendicular to the applied magnetic field, $\mathbf{B}_0$, are shown in Figure 6. Both solid sate ^2H NMR spectra show a single doublet with a splitting of 67 ± 1 kHz. The observation of a single doublet in the solid state ^2H NMR for each sample indicates that the principal C_5-symmetry axis of the $Co(\eta\text{-}C_5D_5)_2$ guests adopts a single orientation relative to the external magnetic field. The observed splitting of *ca.* 67 kHz for crystals oriented with their layers perpendicular to the $\mathbf{B}_0$ field indicates that the C_5 axes of the guest molecules are perpendicular to the external magnetic field $\mathbf{B}_0$ and hence parallel to the host lattice layers. Spectra recorded with the lattice layers parallel to the field, $\mathbf{B}_0$, are inherently more complicated due to the possibility of both static and dynamic guest disorder (Figure 7) and the consequent range of orientations of the deuterium electric field gradient tensor to the applied field. Further studies on the single-crystal ^2H NMR of these materials, which have suggested in-layer packing arrangements entirely consistent with the results of this work, will be published elsewhere.[36,39] For the purposes of this report, it is sufficient to state that the guest molecules are closely packed within the van der Waals planes of the host lattice, the principal molecular axes of the intercalated guest molecules all lie parallel to the layers, but static disorder or molecular motion or both in the *ab* plane give rise to a highly complex structure, as illustrated in Figure 7.

Similar observations on the orientation of $Co(\eta\text{-}C_5H_5)_2$ in metal dichalcogenides have been made in the ^2H NMR studies of $SnS_2\{Co(\eta\text{-}C_5H_5)_2\}_{0.3}$[18,22] and $TaS_2\{Co(\eta\text{-}C_5H_5)_2\}_{0.25}$.[17] For $TaS_2\{Co(\eta\text{-}C_5H_5)_2\}_{0.25}$ however, a second species of $Co(\eta\text{-}C_5H_5)_2$ in a chemically distinct environment was observed; the authors have ascribed this second species to $Co(\eta\text{-}C_5H_5)_2$ molecules with their C_5 molecular axis oriented perpendicular to the host layers. We can obtain no evidence for the presence of this perpendicular orientation in this study.

Conclusion

The intercalation of a range of redox-active organometallic guest molecules into relatively large single-crystal hosts of ZrS_2, SnS_2, and $SnSe_2$ has been achieved. With these samples, we have been able to use X-ray and neutron diffraction techniques to carry out integrated intensity refinements to determine the guest orientation. Oriented single-crystal solid state ^2H NMR experiments have been used to confirm the structures suggested by the diffraction experiments in two cases.

All the guest organometallic sandwich complexes in the intercalates examined were found to adopt an orientation in which the principal molecular axis lies parallel to the crystallographic *ab* plane of the host crystal.

Acknowledgment. We thank Dr Alex C. Hannon for his assistance with the neutron diffraction experiments, Professor M. L. H. Green and co-workers for gifts of the molybdenum and tungsten organometallics, and the SERC for financial support and for access to the neutron diffraction facilities. In addition, H.-V.W. gratefully acknowledges the Rhodes Trust for a scholarship.

Supplementary Material Available: Listings of observed and calculated structure factors for the 1-dimensional refinements (7 pages). Ordering information is given on any current masthead page.

(39) Mason, S. J.; O'Hare, D.; Heyes, S. J. Manuscript in preparation.